Received 28 October 2023
Revised 3 December 2023
Accepted 15 January 2024

Freight train derailment severity prediction: a physics-informed one-dimensional model

Di Kang
Department of Civil and Environmental Engineering, Rutgers University, Piscataway, New Jersey, USA

Steven W. Kirkpatrick
Applied Research Associates Inc., Los Altos, California, USA

Zhipeng Zhang
School of Naval Architecture, Ocean and Civil Engineering, Shanghai Jiao Tong University, Shanghai, China and Department of Civil and Environmental Engineering, Rutgers The State University of New Jersey, Piscataway, New Jersey, USA

Xiang Liu
Department of Civil and Environmental Engineering, Rutgers University, Piscataway, New Jersey, USA, and

Zheyong Bian
Department of Construction Management, University of Houston, Houston, Texas, USA

Abstract

Purpose – Accurately estimating the severity of derailment is a crucial step in quantifying train derailment consequences and, thereby, mitigating its impacts. The purpose of this paper is to propose a simplified approach aimed at addressing this research gap by developing a physics-informed 1-D model. The model is used to simulate train dynamics through a time-stepping algorithm, incorporating derailment data after the point of derailment.

Design/methodology/approach – In this study, a simplified approach is adopted that applies a 1-D kinematic analysis with data obtained from various derailments. These include the length and weight of the rail cars behind the point of derailment, the train braking effects, derailment blockage forces, the grade of the track and the train rolling and aerodynamic resistance. Since train braking/blockage effects and derailment blockage forces are not always available for historical or potential train derailment, it is also necessary to fit the historical data and find optimal parameters to estimate these two variables. Using these fitted parameters, a detailed comparison can be performed between the physics-informed 1-D model and previous statistical models to predict the derailment severity.

Smart and Resilient Transportation
Vol. 6 No. 1, 2024
pp. 72-92
Emerald Publishing Limited
e-ISSN: 2632-0495
p-ISSN: 2632-0487
DOI 10.1108/SRT-10-2023-0008

This research was funded through a contract by the Federal Railroad Administration (693JJ619C000017).

Findings – The results show that the proposed model outperforms the Truncated Geometric model (the latest statistical model used in prior research) in estimating derailment severity. The proposed model contributes to the understanding and prevention of train derailments and hazmat release consequences, offering improved accuracy for certain scenarios and train types

Originality/value – This paper presents a simplified physics-informed 1-D model, which could help understand the derailment mechanism and, thus, is expected to estimate train derailment severity more accurately for certain scenarios and train types compared with the latest statistical model. The performance of the braking response and the 1-D model is verified by comparing known ride-down profiles with estimated ones. This validation process ensures that both the braking response and the 1-D model accurately represent the expected behavior.

Keywords Derailment severity, Hazardous materials, Physics-informed model

Paper type Research paper

1. Introduction

Rail transportation of hazardous materials (hazmat) is typically recognized for its cost-effectiveness and considered a secure and efficient choice for conveying substantial quantities of goods across extensive distances (Wang and Liu, 2022; Zaman *et al.*, 2023). While train derailments resulting in hazmat releases are rare occurrences, they raise significant concerns due to their potential for catastrophic consequences. Hazmat releases caused by train derailments can result in environmental damage, property loss and health risks for nearby communities. A recent example of such an incident took place on February 3, 2023, when a Norfolk Southern train derailed in East Palestine, OH, leading to the release of hazardous combustible chemicals. The ensuing fire further exacerbated the situation, causing destruction to additional cars. The air pollution resulting from this incident had adverse effects on the skin and lungs of residents for several months, with nine monitored chemicals surpassing normal levels (Moore, 2023). Efforts underway to improve safety and reduce train derailment risks include increased rail maintenance, electronically controlled pneumatic brakes adoption and safer tank car designs (Wang and Liu, 2022). Studies suggest organizing tank cars in manifest trains and using suitable configurations can decrease release consequences by up to 50% (Kang *et al.*, 2023; Zhao *et al.*, 2023).

Derailment severity, which refers to the number of cars derailed, holds significant importance in determining the consequences of a train derailment. Understanding the factors influencing derailment severity and precisely estimating it are essential steps to mitigate catastrophic accidents and enhance public safety. Two primary methodologies are used to estimate train derailment severity: statistical models (data driven) and physical models (law driven). Statistical models analyze structured and unstructured empirical derailment data, crafting point estimate models and interval estimation models. These models offer valuable insights into derailment severity (Liu *et al.*, 2013; Martey and Attoh-Okine, 2019; Saccomanno and El-Hage, 1989, 1991; Song *et al.*, 2022). Conversely, physics-based models include one-dimensional (1-D), two-dimensional (2-D) and three-dimensional (3-D) models to simulate train dynamics. These models necessitate a comprehensive depiction of interactions among locomotives and railcars, encompassing suspension elements and wheel-rail contact forces (Pogorelov *et al.*, 2017). Statistical models may have difficulty predicting extreme derailment events that fall outside historical experience, while physical models are able to capture the conditions of a specific train derailment scenario by mathematically describing the physical dynamics of the derailment. However, the detailed 2-D and 3-D physics-based models require complicated calculation processes, and, thus, is not easily applicable for derailment study (Bosso *et al.*, 2021; Singh, 2019; Tang *et al.*, 2023; Xu and Zhai, 2019).

This study uses a simplified approach that involves a 1-D kinematic analysis using data gathered from various derailments. These encompass:

- the length and weight of the rail cars behind the point of derailment;
- the train braking effects;
- derailment blockage forces;
- the grade of the track; and
- the train rolling and aerodynamic resistance.

Since train braking/blockage effects and derailment blockage forces are not always available for historical or potential train derailments, it is also necessary to fit the historical data and determine optimal parameters for estimating these variables. Using these fitted parameters, a comprehensive comparison can be conducted between the physics-informed 1-D model and the preceding statistical model to predict the derailment severity.

The main contributions of this paper include:

- This paper introduces a simplified physics-informed 1-D model designed to enhance understanding of the derailment mechanism. It is anticipated that this model will provide more accurate estimates of train derailment severity for specific scenarios and train types compared to the latest statistical model.
- The accuracy of the braking response and the 1-D model is verified through a comparison of known ride-down profiles with estimated ones. This validation process ensures that both the braking response and the 1-D model accurately represent the expected behavior. Using the simulated annealing (SA) algorithm and Class I derailment data sourced from the Federal Railroad Administration (FRA) Rail Equipment Accident/Incident (REA) database, this paper undertakes the estimation of important parameters within the 1-D model for various train types.
- The presented physics-informed 1-D model is compared to the statistical Truncated Geometric (TG) model, and the results demonstrate that, overall, the proposed 1-D model outperforms the TG model in general.

2. Literature review

Physical models were used in prior research to model train derailment severity, accounting for physical dynamics of the derailment and using that information to estimate the number of derailed cars. Physical models can also help understand how factors, including train speed, tonnage and train length, influence derailment severity from the perspective of physical dynamics.

One type of physical model simulates the longitudinal train dynamics, including traction, braking and longitudinal forces of the coupled cars in the train. A well-established longitudinal train dynamics simulator in North America is the Train Operations and Energy Simulator (TOES™) model developed for and licensed to AAR-member railroads (Andersen *et al.*, 1991, 1992). TOES has been in use for nearly three decades, has been validated many times over and is considered an industry standard for longitudinal train dynamics modeling. A similar 1-D longitudinal dynamics model is the Train Energy and Dynamics Simulator (TEDS) model (Andersen *et al.*, 2012; Sharma and Associates, 2015). TEDS is a more recently developed tool that calculates the in-line train forces and motions under specified track, traction and braking conditions. Additional studies that have developed similar longitudinal dynamics models include Mokkapati and Pascoe (2011) and Wu *et al.* (2014). However, the model proposed in Mokkapati and Pascoe (2011) is not generally used since it is based on braking function performed by the on-board computer of a positive train control system. These models have been specifically designed for analyzing train dynamics under normal operating conditions. However, they are not suitable or capable of analyzing the response that occurs after a derailment is initiated.

Another type of physical model includes 2-D and 3-D models of the individual vehicle dynamics, including additional mechanics such as the wheel-rail interaction forces, suspension dynamics and derailment kinematics. For example, Toma developed a detailed 2-D multi-body simulation (MBS) train derailment model for his Ph.D. thesis project (Toma, 1998). Toma's model includes significant features from a longitudinal model such as the traction, braking and coupler forces for the cars on the track. Once derailed, the cars are subject to 2-D motions with a velocity-dependent ground friction model, impact forces and uncoupling of cars based on strength and displacement limits. The primary limitations of Toma's model are the simplifications necessary in an MBS model for calculating impact behaviors and the constraint that the model is only 2-D. Other 2-D MBS derailment studies include Paetsch *et al.* (2006) and Jeong *et al.* (2007).

As a result of the complexity of post derailment behaviors, more recent derailment models have relied on 3-D computational solvers to simulate the response. An example of this type of model for simulating train derailments using the LS-DYNA finite element solver was performed by Kirkpatrick (2021). The fully 3-D finite element model allows for many additional complex derailment mechanics such as deformation and failure of components and connections (e.g. truck separations and breakup, coupler failures), realistic impact scenarios between derailed cars and derailment conditions on slopes, elevated rail berms, etc. For the purpose of investigating the factors that influence derailment severity, the 3-D modeling approach was more complex and computationally intensive than required. In contrast, 1-D models are less complex and more computationally efficient and are capable of capturing train derailment dynamics. Kirkpatrick *et al.* (2021) originally introduced the concept of a simplified 1-D model. In this paper, we further develop and elaborate on their initial work, presenting a comprehensive and detailed mathematical model that extends and refines their original ideas.

3. Physics-informed 1-D model

The proposed 1-D model operates as a time-stepping algorithm, necessitating specific inputs. These inputs comprise details about the residual train (i.e. the train behind the derailment point), encompassing the number of cars, individual car weights and car lengths. Additional features, like a trailing locomotive, can be incorporated as well. The derailment speed and time histories for the braking and blockage forces and rolling resistance are specified as input conditions at the start of the analysis. For derailments with trailing locomotives, the weight, position and locomotive brake ratio are all specified.

At each time step, the braking, blockage and train resistance forces are updated and applied to the cars behind the point of derailment (POD) to calculate the deceleration rate. The equations of motion for the residual train are solved with a computational approach. At each time step, the sum of the forces acting on the train is calculated (braking, blockage, rolling resistance and gravitational). The distance traveled, residual length and residual train mass are also updated. The algorithm then steps through time analyzing the motions of the residual train (the portion of the train behind the point of derailment). This process is solved by incremental time steps up to the point where the residual train comes to rest. A general flowchart for the model methodology is provided in Figure 1.

Further details regarding the various components of the model are explained in the subsequent sections.

3.1 Train braking effect

Rather than develop a model for the air brake system from first principles, a simplified approach is adopted that applies data obtained from various derailments. Three derailments are selected that had different residual train lengths, and trailing

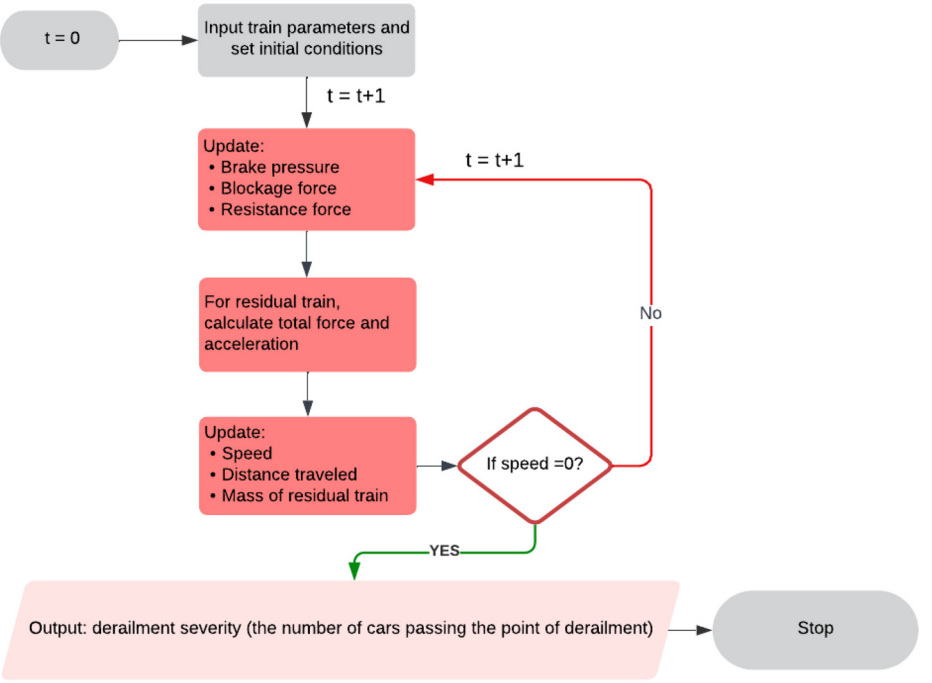

Figure 1.
Physics-informed 1-D model flowchart

Source: Authors' own work

locomotives with event recorders that provided data on the brake pressure and deceleration response of the cars behind the derailment. The residual train length is defined as the length of the train behind the POD and is an important parameter since it influences how rapidly the air brakes are applied. These three derailments are (Brosseau, 2014):

(1) Aliceville, AL, 11/7/2013; Loaded unit oil train, 90 cars behind POD.
(2) Brainerd, MN; 7/10/2011; 27 mph; Loaded unit coal train, 56 cars behind POD.
(3) Wagner, MT; 2/13/2013; 37 mph; Loaded unit grain train, 17 cars behind POD.

The brake cylinder pressure histories for the three derailments are depicted in Figure 2 (solid line). All three are characterized by a steady increase in pressure during application combined with a transition phase at the beginning and end of brake application. The primary difference in the curves appears to be a shift in the time for which the increase in brake pressure occurs. This shift is correlated with the residual length of the train behind the POD, where a shorter residual train length (Wagner, 17 cars behind POD) results in an earlier application of brakes, while a longer residual train length (Aliceville, 90 cars behind POD) results in a delayed brake application.

To analyze the specific responses in these three derailments, the recorded brake application curves can be applied. However, in the absence of this data for the majority of derailments, an approach has been devised to estimate a brake application curve for others. This involves applying a time shift to a baseline pressure curve (from the Brainerd

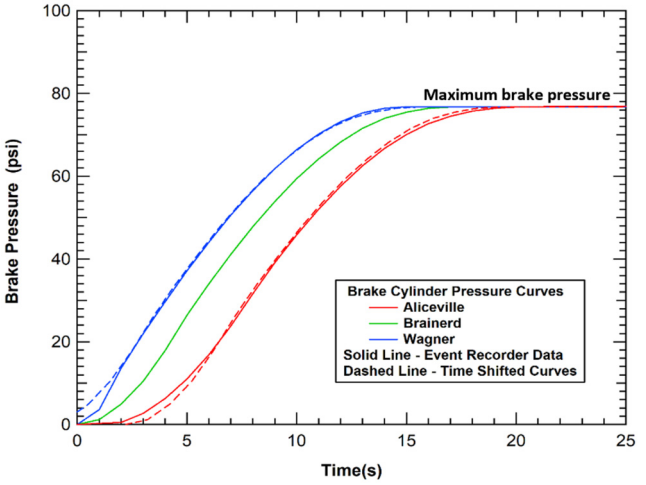

Source: Authors' own work

Figure 2. Comparison of the time-shifted brake pressure curves and event recorder curves

derailment). The equation used to implement the time shift in the brake application curves for different derailments is:

$$T_s = T_0 + \left[(N_c L_C - L_0)/1150\right] \tag{1}$$

where

T_s = the shifted time (s);
T_0 = the baseline (reference) time (s);
N_c = the number of cars in the residual train;
L_C = the average length of the cars in the residual train (in feet); and
L_0 = the baseline (reference) residual train length (in feet).

Equation (1) effectively shifts the time based on the difference in the length of the residual train divided by the sound speed in the air pipe (1,150 ft/s). For the corrections performed here, the reference residual train length used for Brainerd is 2,852 ft. For example, for Aliceville derailment, according to equation (1), the shifted time of brake pressure curve is (91 car × 59.3 ft – 2,852 ft)/1,150 ft/s, which is 2.2 s. This means the brake pressure curve of Aliceville derailment can be approximately obtained by shifting the base derailment, Brainerd derailment, by 2.2 s. A comparison of the time shifted brake pressure curves with the event recorder curves for the Aliceville and Wagner derailments is shown in Figure 2. The comparison shows that the time-shifted curve serves as a reliable approximation of the actual brake application behavior and represents a suitable approach for estimating braking in derailments where brake pressure data is unavailable.

An additional feature incorporated into the brake application model within the 1-D model is the inclusion of a brake application delay time. The brake application curves, depicted in Figure 2, uses a derailment initiation reference time from the event data recorder (time = 0). This time is determined from the brake pressure change that initiates the onset of emergency braking. However, this is the time when a separation occurs in the brake pipe rather than the time when an initial car derails.

In a typical derailment, initiation occurs due to some failure in the rail, equipment or an excess of lateral loads at the wheel-rail interface. The initial cars that derail are usually still connected to the leading and trailing cars, aligning closely with the original rail orientation. A delay typically exists between the initial wheel derailment and the time when additional forces on the derailed cars lead to a failure of the coupled connection, resulting in separation from the leading cars ahead of the point of derailment. It is typically only after this delay and coupler separation that the brake pipe will be broken, initiating the emergency brake. As a result, a brake application delay time is added to shift (delay) the brake application curve from the time of the derailment initiation. The magnitudes of these brake application delay times are further discussed in the model validation analyses.

The braking forces are assumed to be proportional to the brake application. This paper uses an emergency braking force of 7,800 lbs brake force per car at full pressure (Lovette and Thivierge, 1992). This level corresponds to a 3% brake ratio for a 263 K gross rail load (GRL) loaded car and a 12% brake ratio for a 65 K light-weight empty car. Similarly, a 9% brake ratio is assumed to be typical for locomotives in emergency braking with an application that follows the same pressure curve.

3.2 Derailment blockage force

The subsequent factor in the physics-informed 1-D model is the derailment blockage force. This force represents the in-line train force generated by the derailed cars and acting on the remaining cars on the rail behind the POD. The kinematics of a car approaching and passing the POD in a derailment is illustrated in Figure 3. The blockage resistance is a composite of the increased rolling or sliding resistance between the car and ground after leaving the rail and the forces resulting from impacts against a pileup of previously derailed cars in the forward portion of the derailment. The force is either transmitted through the draft gear or by any point of contact resulting from impacts between cars. The magnitude of the force

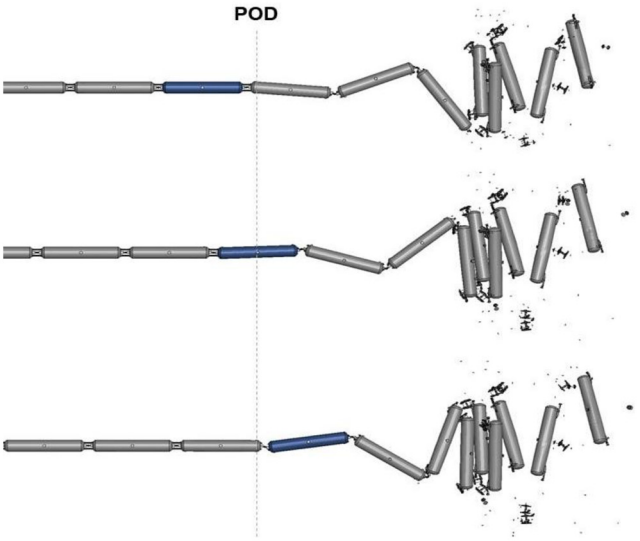

Source: Authors' own work

Figure 3.
Example kinematics of a car passing the POD

transmitted longitudinally from the derailed cars will also be a function of the continually changing alignment of cars resulting from the lateral buckling of derailed cars.

Previous studies have examined and analyzed the magnitude of this blockage force. In an analysis conducted by Brosseau (2014), several derailments were studied by comparing the deceleration response to the calculated deceleration resulting from braking alone. The calculated blockage forces in these instances ranged between 500 and 650 kips. Similarly, an analysis of the Lac Mégantic derailment (Transportation Safety Board of Canada, 2014) found an average blockage force of approximately 400 kips. Notably, in this case, the train was a runaway with no braking applied, meaning the blockage force was solely responsible for halting the motion of the cars on the rail behind the point of derailment.

While the blockage force is not expected to be a smooth profile due to the buckling and impact behaviors of the cars (Transportation Safety Board of Canada, 2014), it is commonly approximated as a smooth force in models, as depicted in Figure 4. In addition, there exists a potential period at the initiation of the derailment where the cars ahead of the derailment provide a traction force until separation occurs. Thus, the blockage is modeled with a delay time before blockage forces begin, a ramp time over which the blockage force is linearly increased and then a steady state when blockage force is fully developed. This blockage force is applied in the model as a force fixed at the POD acting on the remaining cars (mass) on the rails behind that position. The assumption made in this paper is that a pileup is not formed until there is a separation between cars. Therefore, the blockage delay and the breaking delay are assumed to be coupled to each other and share the same value.

3.3 Train resistance

The final set of forces included in the model is the standard train resistance forces. Gravitational acceleration is added to a train on either an uphill or downhill grade. A model for the remaining train resistance is also added based on existing models (Hay, 1982). Davis equation, which is a well-known resistance formula with a quadratic form in velocity, is used in this paper:

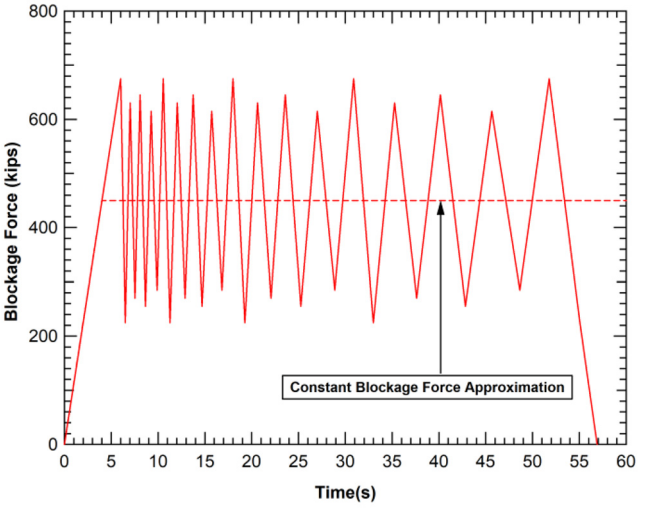

Source: Authors' own work

Figure 4.
Schematic illustration of the blockage force profile in a derailment

$$R = A + Bv + Cv^2 \tag{2}$$

with constant coefficients derived from experimental work conducted by Davis (1926). It has multiple variants known as the Modified Davis and Adjusted Davis equations. The resistance calculations of the Davis equation are commonly defined as a force per unit train weight. In the Davis equation, the constant term A represents the journal rolling resistance. The second term represents the flange resistance and is proportional to the train speed. The final term is the wind resistance and is proportional to the square of the train speed. For the model, we use the following values for the resistance:

$$A = 1.3 + \frac{29}{w} \quad (\text{lbs/ton}) \tag{3}$$

$$B = 0.045 \quad (\text{lbs/ton} - \text{mph}) \tag{4}$$

$$C = 5.2 \quad \left(\text{lbs/ton} - \text{mph}^2\right) \tag{5}$$

where w is the axle load in tons. These coefficients produce the resistance magnitudes shown in Figure 5 for a 263k GRL-loaded freight car. An assessment of these resistance forces indicates that they are most significant at high speed and, as a result, have little effect on most derailments.

As illustrated in Figure 1, we can update various parameters such as total force, acceleration, speed, distance traveled and residual train mass that has not derailed. The residual train mass can be readily calculated based on distance traveled and the known point of derailment.

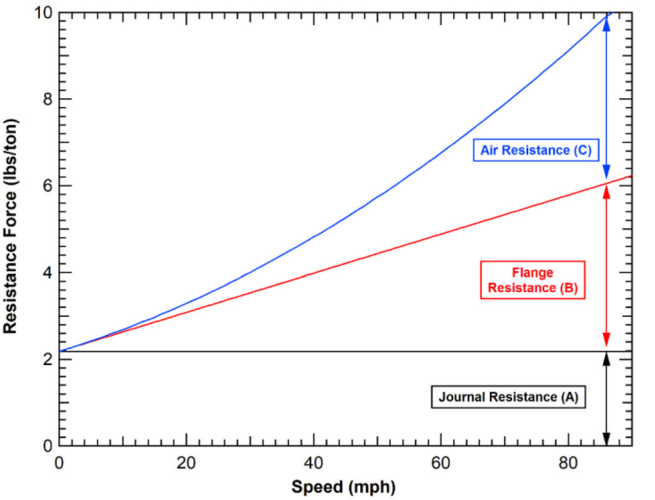

Source: Authors' own work

Figure 5.
Resistance model for a conventional freight train

4. Model validation

This paper includes model validation for both train braking and the overall model. The primary validation approach involves assessing the response for a set of derailments where quantitative information about the derailment kinematics is known, typically from event recorder data. The primary data of interest for this assessment is the ride-down velocity profile, representing the time history of the train velocity from the derailment initiation to the point where all train cars come to rest. By comparing known train ride-down profiles to predicted behaviors, we can effectively validate the model. The ride-down profiles over a range of derailment conditions can only be matched if the various contributions to the longitudinal forces are all accurately included in the model.

Train braking is often the most significant component of the longitudinal forces acting on the train in many derailments. Therefore, it is critical to independently evaluate this aspect of the model. Following a derailment, a train typically loses stability and deviates from its intended path, leading to a separation of the train into two parts due to the forces and dynamics involved during the derailment process. Usually, the 1-D model is applied to the portion of the train behind the POD. However, the 1-D model can be applied to the part of the train ahead the POD (still on the rails) to validate the performance of the braking response. In this scenario, no blockage force is present, allowing for an assessment of the emergency braking model in this analysis.

For validation of the braking response, eight train derailments are selected for which the event recorder data are available from a leading locomotive ahead of the POD. The derailment information input for braking analyses is shown in Table 1. This data is used to calculate the ride down profile for the leading cars remaining on the rails ahead of the POD. The comparison between event recorder data and the simulated train speed is shown in Figure 6, which shows that the braking model is capable of accurately reproducing the ride-down response for the lead section of the train in each derailment.

To validate the physics-informed 1-D model for the train behind the POD, five derailments are selected that had different residual train lengths and trailing locomotives

Incident date	Location	Train type	Speed (mph)	No. cars ahead of POD	No. leading locos	Avg. car weight (kips)	Grade (%)
6/19/2009	Cherry Valley, IL	Mixed freight train	36	60	2	264	−0.26
4/30/2014	Lynchburg, VA	Loaded unit oil train	24	71	2	269	−0.10
3/10/2017	Graettinger, IA	Loaded unit ethanol train	28	80	1	254	0.20
2/16/2015	Mount Carbon, WV	Loaded unit oil train	33	3	2	272	−0.05
9/19/2015	Lesterville, SD	Loaded unit ethanol train	10	97	1	257	0.00
8/2/2017	Hyndman, PA	Mixed freight train	31	32	5	111	−1.43
8/12/2019	Carey, OH	Loaded unit sand train	23	9	2	286	−0.29
2/8/2020	Sesser, IL	Loaded unit coal train	43	99	2	286	0.18

Source: Authors' own work

Table 1. Derailment information for braking model validation analyses

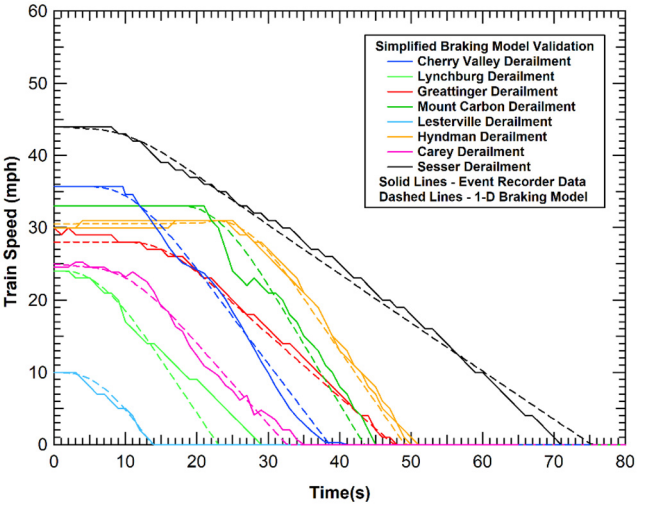

Figure 6.
Validation of the braking force model for the part of the train before the point of derailment

Source: Authors' own work

with event recorders (Table 2). Such residual length variation tests the relative importance of different aspects of the model. For example, the blockage force is applied to the POD. As a result, the blockage forces are much more significant for a small residual train length (less mass behind the POD) than they will be for a long residual train.

The event recorder data for these trailing locomotives provided data on the brake pressure and deceleration response of the residual cars. Most of the input parameters are known characteristics of the derailment conditions and equipment involved. The two parameters that are developed for these analyses are the blockage force and the braking and blockage delay time. The blockage force level is obtained by a fitting analysis as a function of various derailment parameters as described below. The braking and blockage delay time

Parameter	Units	Aliceville, AL 11/7/2013	Brainerd, MN 7/10/2011	Graettinger, IA 3/10/2017	Wagner, MT 2/13/2013	Casselton, ND 12/30/2013
Derailment speed	MPH	39	27	29	37	43
Number of cars beyond the point of derailment	Each	91	59	106	20	109
Length of cars	Feet	59.3	54.0	59.9	57.0	59.6
Avg. car weight	kips	260	284	254	286	252
Trail locos	Each	1	1	1	1	1
Residual train mass	M lbs	23.8	16.9	20.7	5.0	28.0
Blockage force	kip	472	466	469	511	461
Braking and blockage delay	s	5	14	10	3	0
Blockage ramp time	s	4	4	4	4	0
Car braking force	lbs	7,800	7,800	7,800	7,800	7,800
Grade	Percent	−0.35	0	−0.14	0.30	0.10

Table 2.
Derailment information for the 1-D derailment model validation analyses

Source: Authors' own work

for these five specific accidents is set to match the conditions of the curve obtained from the event recorder data and accident severity.

The comparison of the results for the ride down velocity profile from the 1-D analyses and event recorder data from the derailment is shown in Figure 7, which shows a good agreement in the calculated and measured ride down profiles indicating that the model is accurately capturing the longitudinal forces acting on the residual train during the derailment.

In addition to providing a validation of the model, the analyses of these derailments provide some interesting insights into the derailment behaviors. First, the average blockage force for all five derailments is 475 kips. This is the equivalent of the fully developed braking force for approximately 60 freight cars. Thus, the blockage has a very significant effect on stopping the residual train. A second insight into the derailment behaviors is that the brake application delay time varies between 0 and 14 s in these derailments. The 0 s delay time was for Casselton where the derailment was initiated by a collision with equipment from a derailment on an adjacent track. For this derailment, the operator placed the train into emergency seconds prior to impact with the obstruction across the track (National Transportation Safety Board, 2017). In more typical derailments, the delay time results in several cars being pulled through the point of derailment before a separation in the train occurs and the emergency braking is initiated. For example, the Brainerd derailment with a 14 s delay time results in approximately 10 cars being pulled past the point of derailment on the track prior to the initiation of emergency braking. Thus, this delay has a significant impact on the overall derailment severity.

The primary model validation, described above, is performed by a detailed comparison of the model against data for events where the quantitative derailment kinematics is known. However, the magnitude of the delay time for the braking and blockage force are varied to match the measured derailment behavior. A secondary model validation has been performed on a larger set of derailments using the model with a fixed set of input parameter values. A difficulty with performing this secondary validation is that the details of the train consist makeup is not known for most revenue train derailments. Since the weight of the

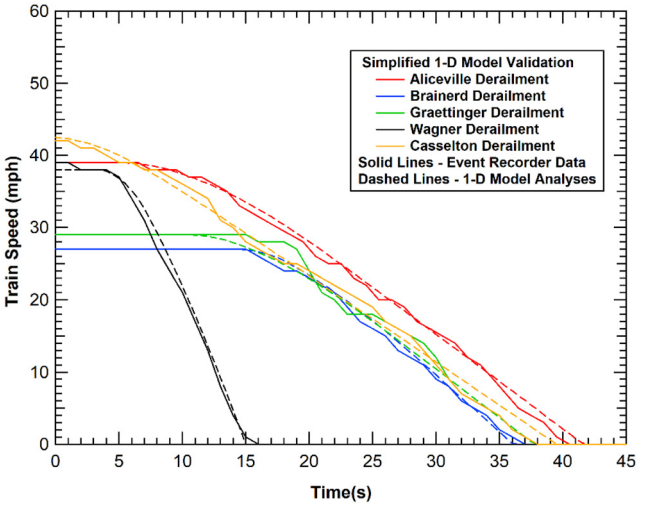

Source: Authors' own work

Figure 7. Validation of the 1-D derailment model for scenarios with known ride-down profiles

cars both within and behind the POD can have a significant influence on the derailment severity, the derailments selected for the second validation analyses are primarily unit trains where the consistency is easily determined.

A set of 442 train derailments are identified from various sources that span a range of derailment speeds, residual train lengths and derailment severities. The predicted model severity is plotted against the observed derailment severity for the secondary model validation cases in Figure 8. The comparison shows a good correlation of the model with the observed derailment behavior. Any single derailment may have a predicted severity that is higher or lower than the observed severity by several cars. This magnitude of variation is expected due to anticipated variability in factors such as braking or blockage delay and site characteristics. However, the trend and average severities are in good agreement.

For the analyses shown in Figure 8, the blockage force and delay times applied are obtained using fitting functions to minimize the mean absolute error (MAE) in predicted severity. For example, the delay time is determined by a linear function of the derailment speed, grade, car weight and trailing tons. To demonstrate the importance of this, Figure 9 plots the delay time that would be required to match the observed severity of each derailment plotted against the derailment speed. The comparison shows a clear trend of shorter delay times at higher speed. This makes physical sense because at high speed, cars are more rapidly pulled past the point of derailment, developing larger ground resistance forces. Similarly, the delay time is shorter for heavier cars which would also have higher ground resistance force levels. The delay time is also increased on uphill grades and reduced on downhill grades. The blockage force is affected by the lateral buckling of the cars in the consist as they enter the pileup. Thus, longer and heavier cars result in an increase in the blockage force. The blockage force is also found to increase on uphill grades. The magnitude of these effects for loaded unit trains can be seen by the comparison of the blockage force levels in Table 2.

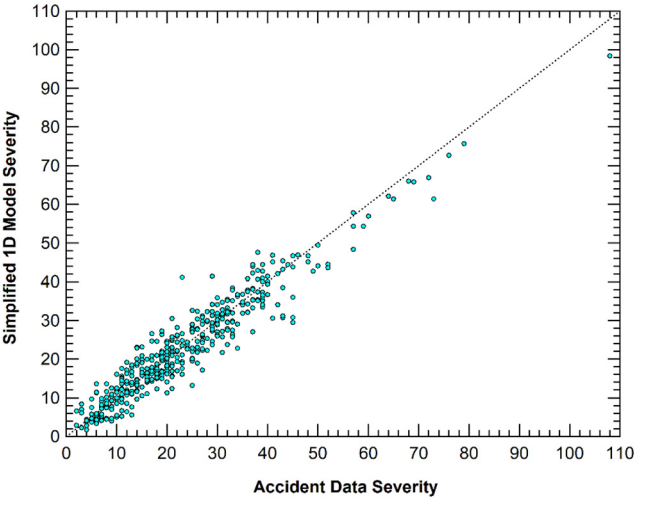

Source: Authors' own work

Figure 8.
Validation of the 1-D model against derailment severity data for known train configurations

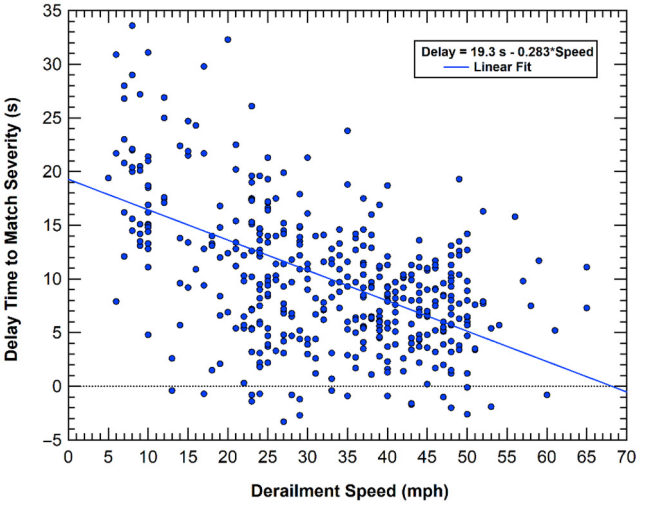

Source: Authors' own work

Figure 9.
Assessment of delay times versus derailment speed using the 1-D model

5. Parameter estimation and performance comparison

In the previous section, two model validation approaches are used to demonstrate a general validation and provide a comprehensive understanding of the proposed 1-D model. However, further analyses are essential to establish estimations for the unknown parameters in the 1-D model. In addition, a crucial aspect involves comparing the performance of the 1-D model with that of the statistical model to achieve a more comprehensive evaluation.

This section uses derailment data obtained from the FRA REA/Incident Form 6,180.54, documenting freight train derailments on the main tracks of Class I railroads spanning the period from 1996 to 2018. The data set contains various parameters, including derailment location, the number of derailed locomotives and cars, gross tonnage, cause group, derailment speed, train type and train composition. Since the data set lacks grade information, it is assumed in this section that all derailments occur on a flat track. The optimization of parameters for braking/blockage delay and blockage force aims to minimize the MAE between estimated and observed derailment severity.

Similar to the outliers identified by the statistical model (Li *et al.*, 2023), the proposed 1-D model exhibits certain instances of derailments categorized as "low-severity outliers" and "high-severity outliers." These outliers are attributed to the focus of the 1-D model on derailment incidents following the physical mechanism of an unstable lateral buckling derailment, commonly associated with broken rail derailments and similar events. Consequently, the 1-D model does not account for outlier behaviors, such as broken wheel single-car derailments or a long string of empty cars in a stationary train knocked over by a high wind event. As a result, this analysis excludes derailments where the number of derailed cars falls below 0.1 times the derailment speed (in mph) or exceeds 1.6 times the derailment speed.

Assuming an average car length of 59 feet, with braking delay and blockage delay set at 12 s, a blockage force of 400 kips, grade is 0 and a blockage ramp

time of 4 s, Figure 10 shows the comparison of the performance of 1-D model with or without outliers. Remarkably, the exclusion of outliers leads to a notable improvement in the estimation performance of the 1-D model, as evidenced by an increase in the R-squared value from 0.22 to 0.63. Upon excluding all outliers, the analysis shows a total of 5,186 manifest train derailments, 274 empty unit train derailments and 1,448 loaded unit train derailments.

Obtaining specific information for each derailment, such as blockage force and blockage/braking delay, is not always feasible. Therefore, it becomes crucial to determine optimal parameters for estimating blockage/braking delay and blockage force (equations (6)–(7)). The paper uses the SA algorithm, which is a probabilistic optimization technique inspired by the annealing process in metallurgy. SA explores the solution space by considering both superior and inferior solutions throughout the simulation, gradually diminishing the acceptance of suboptimal solutions as the algorithm advances. In this study, the SA algorithm is used to identify near-optimal solutions for estimating these parameters.

$$\delta_{\text{Brake}} = \delta_{\text{Block}} = a_0 + a_1 \times v_{\text{D}} + a_2 \times w_{\text{car}} + a_3 \times w_{\text{Res}} \tag{6}$$

$$BF = b_0 + b_1 \times w_{\text{car}} \tag{7}$$

where

δ_{Brake} = the braking delay (s);
δ_{Block} = the blockage delay (s);
BF = blockage force (kip);
v_{D} = derailment speed (mph);
w_{car} = the average car mass (kip);
w_{Res} = the residual train mass (kip); and
$a_0, a_1, a_2, a_3, b_0, b_1$ = parameters need to be estimated.

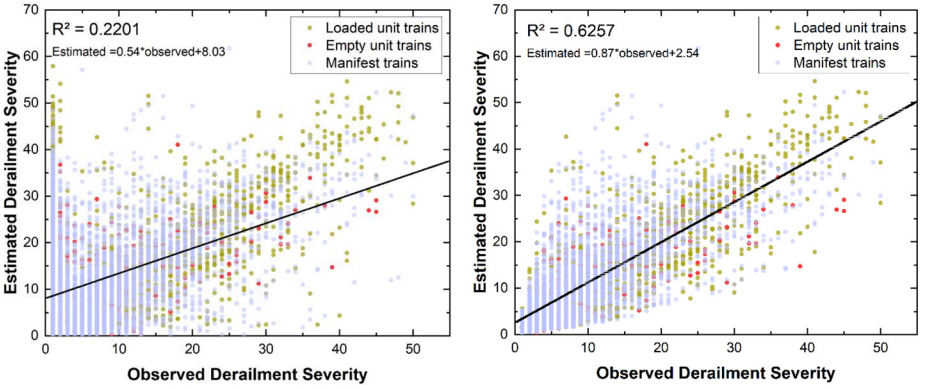

Figure 10.
The comparison between estimated severity and observed severity using the 1-D model (a) data with outliers and (b) data without outliers

Source: Authors' own work

Algorithm 1: Algorithm to estimate parameters for 1D model using simulated annealing

Input: Derailment information for each historical derailment (assume N of derailments included) that happened from 2006 - 2018 (including the number of cars beyond the point of derailment, car mass, the total number of cars in the train, car length in feet, the number of locomotives and the weight for each of the locomotive, train consist, the blockage ramp time, emergency braking force per car at full pressure, derailment speed, brake ratio, flange resistance, wind resistance, and brake pressure curve.

Output: Optimal values for parameters to estimate brake delay and blockage force in the 1D model.

Initialize a parameter set S, and set $S_{\text{best}} = S$.
Calculate the $MAE(S)$ using the proposed 1D model with the parameter set S.
Set $MAE_{\text{best}} = MAE(S) = M$, where M is a large number.
Generate a neighborhood parameter set $S' = Neighborhood(S)$
while $t > t_{Final}$ **do**
  for $j \leftarrow 1$ **to** J_0 **do**
    for $i \leftarrow 1$ **to** N **do**
      Run the 1D model using the parameter set S';
    end
    Calculate $MAE(S')$;
    if $MAE_{best} > MAE(S')$ **then**
      $MAE_{best} \leftarrow MAE(S')$
      $S_{\text{best}} = S'$
    end
    if $MAE(S') < MAE(S) || e^{\left(-\frac{MAE(S')-MAE(S)}{t}\right)} > random(0,1)$ **then**
      $S = S'$
      $MAE(S) = MAE(S')$
    end
    Generate a neighborhood parameter set S' around S for the next time step.
  end
  $t = t \times \Delta t \quad (\Delta t < 1)$
end

Using the data excluding outliers and following Algorithm 1, we estimate the optimal parameter values for equations (6)–(7) for loaded unit trains, empty unit trains and manifest trains. The estimated values are presented in Table 3. By plugging in the average values for

variables in equations (6)–(7), the average braking/blockage delay times, as well as the average blockage force, are also calculated and showed in Table 3. The results indicate that loaded unit trains typically experience the highest blockage force and delay time, whereas empty unit trains generally encounter the lowest delay time and blockage force, with manifest trains falling in between. While a_3 for empty unit trains and a_2 for manifest trains are positive, they are almost zero. Since a_2 and a_3 are both parameters for weight variables, they compensate each other to achieve optimal estimation.

To thoroughly evaluate the efficacy of the proposed 1-D model, this paper conducts a comparative analysis with the TG model introduced by Li *et al.* (2023), representing the latest statistical model estimating derailment severity. The comparison of the overall MAE is shown in Table 4. In addition, the derailment incidents are categorized into five severity levels. The MAE for both the 1-D model and the TG model in estimating each severity level category is calculated.

Table 4 shows that the 1-D model consistently outperforms the TG model in terms of overall estimation accuracy for all train types, exhibiting lower MAE values. This superiority in accuracy across various types of trains underscores the enhanced estimation performance of the 1-D model. Notably, the 1-D model excels in estimating loaded unit trains, characterized by larger train lengths and gross tonnage, making them more susceptible to severe derailments. In addition, Figure 11(a) further demonstrates that, for loaded unit trains, the 1-D model excels over the TG model in estimating extreme derailments (derailment severity > 10) that fall outside historical experience. The 1-D model achieves this by mathematically describing the physical dynamics of a derailment, enabling it to better capture the conditions of specific train derailment scenarios.

Figure 11(b) and Figure 11(c) indicate that the 1-D model falls short compared to the TG model in estimating derailment severity larger than 20 for manifest trains and empty unit trains. However, the 1-D model consistently outperforms or achieves comparable accuracy to

Table 3.
Results for 1-D model parameters estimated values for parameters in 1-D model

Parameters	Loaded unit trains	Empty unit trains	Manifest trains
a0	2.37E + 01	8.42E + 00	1.52E + 01
a1	−2.84E − 01	−7.90E − 02	−3.32E − 01
a2	−5.59E − 04	−1.53E − 03	3.73E − 04
a3	−1.65E − 08	8.48E − 08	−1.02E − 07
b0	4.47E + 00	7.90E − 01	2.37E + 00
b1	3.48E + 00	3.90E + 00	2.58E + 00
MAE	3.80	4.19	3.80
Average braking and blockage delay time (s)	14.55	5.17	8.8
Average blockage force (kip)	464	127	224

Note: *Assume the blockage ramp time is 4 s and the average car length is 59 feet
Source: Authors' own work

Table 4.
Comparison of MAE obtained by 1-D model and TG model

Train types	1-D model	Truncated geometric model
Loaded unit train	3.80	4.20
Empty unit train	4.19	4.40
Manifest train	3.80	3.94

Source: Authors' own work

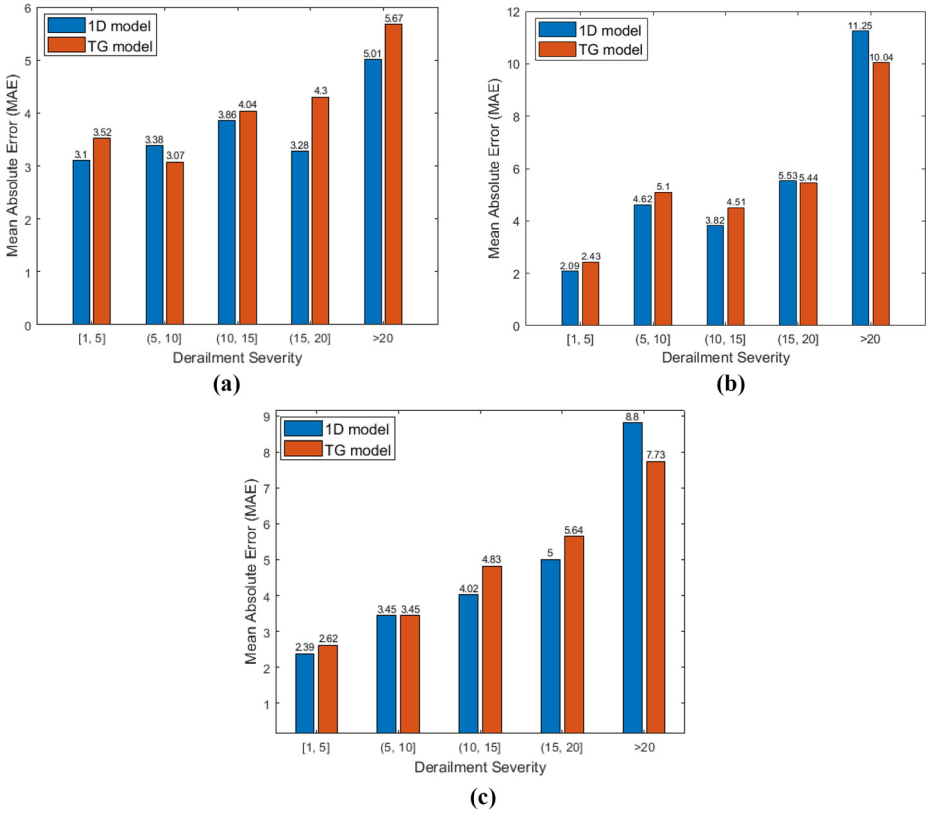

Figure 11. Comparison between 1-D model and TG model for different severity levels for (a) loaded unit trains (b) empty unit trains and (c) manifest trains

Source: Authors' own work

the TG model when estimating derailments in other categories. The performance of the 1-D model faces challenges in extreme cases for manifest trains, likely due to the mixed weight composition of these trains. The 1-D model assumes consistent weights for the cars due to data limitations, which is not always hold true. Similarly, accurate estimation of extreme cases for empty unit trains proves challenging due to the limited occurrence of such events within the study period. Within the study period, only 33 empty unit train derailments involved more than 20 derailed cars, resulting in limited data availability for effective modeling. In addition, the data set lacks grade information, but most severe derailments occurred on downhill grades. This absence of grade data impedes the optimal performance of the 1-D model.

6. Conclusions and future study

This paper introduces a physics-informed 1-D model for estimating train derailment severity. The model is validated through two approaches. Parameters for braking/blockage delays, as well as blockage force, are estimated using historical derailment data spanning over two decades. The following conclusions are drawn based on the severity estimation results obtained by comparing the TG model and the 1-D model:

- The FRA REA/Incident Form 6,180.54 database contains outliers that do not represent typical derailments or primary risk factors for tank car punctures and hazmat releases. These outliers adversely affect the estimation performance of the 1-D model.
- The 1-D model consistently outperforms the TG model in terms of MAE across all train types. This consistent superiority underscores the effectiveness of the 1-D model in accurately estimating derailment severity.
- The 1-D model excels in capturing specific characteristics of train derailment scenarios by mathematically representing the involved physical dynamics. However, despite its general superiority over the TG model, the 1-D model faces limitations due to data constraints. These constraints can impact the performance of the 1-D model in particular scenarios.

For future studies, it would be advantageous to develop specific parameters for the 1-D model that target derailments with distinct causes. This approach involves constructing the 1-D model with customized and estimated parameters designed for different derailment causes. By doing so, a more targeted and precise analysis of derailment severity estimation can be achieved.

References

Andersen, D.R., Mattoon, D.W. and Singh, S.P. (1991), "Revenue service validation of train operations and energy simulator (TOES)- version 1.5 part I: conventional unit coal train", AAR Technical Center.

Andersen, D.R., Mattoon, D.W. and Singh, S.P. (1992), "Revenue service validation of train operations and energy simulator (TOES) version 2.0: Part II: intermodal train", AAR Technical Center.

Andersen, D.R., Booth, G.F., Vithani, A.R., Singh, S.P., Prabhakaran, A., Stewart, M.F. and Punwani, S.K. (2012), "Train energy and dynamics simulator (TEDS): a state-of-the-art longitudinal train dynamics simulator", *Rail Transportation Division Conference*, pp. 57-63, doi: 10.1115/RTDF2012-9418

Bosso, N., Magelli, M. and Zampieri, N. (2021), "Development and validation of a new code for longitudinal train dynamics simulation", *Proceedings of the Institution of Mechanical Engineers, Part F: Journal of Rail and Rapid Transit*, Vol. 235 No. 3, pp. 286-299, doi: 10.1177/0954409720923497.

Brosseau, J. (2014), "Analysis and modeling of benefits of alternative braking systems in tank car derailments", Report R-1007; Issue Report R-1007, Transportation Technology Center.

Davis, W.J. (1926), *The Tractive Resistance of Electric Locomotives and Cars*, General Electric, MA.

Hay, W.W. (1982), *Railroad Engineering*, John Wiley and Sons, New York, NY.

Jeong, D.Y., Lyons, M.L., Orringer, O. and Perlman, A.B. (2007), "Equations of motion for train derailment dynamics", pp. 21-27, doi: 10.1115/RTDF2007-46009

Kang, D., Zhao, J., Tyler Dick, C., Liu, X., Bian, Z., Kirkpatrick, S.W. and Lin, C.-Y. (2023), "Probabilistic risk analysis of unit trains versus manifest trains for transporting hazardous materials", *Accident Analysis and Prevention*, Vol. 181, p. 106950, doi: 10.1016/j.aap.2022.106950.

Kirkpatrick, S.W. (2021), "An evaluation of derailment mechanics and derailment analysis methodologies", *ASME/IEEE Joint Rail Conference*, p. 84775.

Kirkpatrick, S.W., Liu, X. and Dick, C.T. (2021), "Development of a simplified derailment model for investigations of derailment severity".

Li, W., Bian, Z. and Liu, X. (2023), "Statistical analysis of train derailment severity for unit trains versus manifest trains", *Transportation Research Record: Journal of the Transportation Research Board*.

Liu, X., Saat, M.R., Qin, X. and Barkan, C.P.L. (2013), "Analysis of U.S. freight-train derailment severity using zero-truncated negative binomial regression and quantile regression", *Accident Analysis and Prevention*, Vol. 59, pp. 87-93, doi: 10.1016/j.aap.2013.04.039.

Lovette, P.M. and Thivierge, J. (1992), "Train make-up manual", *AAR*.

Martey, E.N. and Attoh-Okine, N. (2019), "Analysis of train derailment severity using vine copula quantile regression modeling", *Transportation Research Part C: Emerging Technologies*, Vol. 105, pp. 485-503, doi: 10.1016/j.trc.2019.06.015.

Mokkapati, C. and Pascoe, R.D. (2011), "A simple and efficient train braking algorithm for PTC systems", *American Railway Engineering and Maintenance-of-Way Association*.

Moore, A. (2023), "After Ohio train derailment, expert warns of potential health impacts from air pollution", *College of Natural Resources News*, available at: https://cnr.ncsu.edu/news/2023/03/ohio-train-derailment-health-impacts-air-pollution/

National Transportation Safety Board (2017), "BNSF railway train derailment and subsequent train collision, release of hazardous materials, and fire—Casselton, North Dakota", NTSB/RAB-17/01; Railroad Accident Brief.

Paetsch, C.R., Perlman, A.B. and Jeong, D.Y. (2006), "Dynamic simulation of train derailments", *ASME International Mechanical Engineering Congress and Exposition*, pp. 105-114, doi: 10.1115/IMECE2006-14607

Pogorelov, D., Yazykov, V., Lysikov, N., Oztemel, E., Arar, O.F. and Rende, F.S. (2017), "Train 3D: the technique for inclusion of three-dimensional models in longitudinal train dynamics and its application in derailment studies and train simulators", *Vehicle System Dynamics*, Vol. 55 No. 4, pp. 583-600.

Saccomanno, F.F. and El-Hage, S. (1989), "Minimizing derailments of railcars carrying dangerous commodities through effective marshaling strategies", *Transportation Research Record*, Vol. 1245 Nos 34/51, pp. 39-41.

Saccomanno, F.F. and El-Hage, S.M. (1991), "Establishing derailment profiles by position for corridor shipments of dangerous goods", *Canadian Journal of Civil Engineering*, Vol. 18 No. 1, pp. 67-75.

Sharma and Associates (2015), "Validation of the train energy and dynamics simulator (TEDS)", FRA Report No. DOT/FRA/ORD-15/01.

Singh, S.K. (2019), "A Full-Vehicle motion simulator for railways applications", *Multibody Dynamics 2019: Proceedings of the 9th ECCOMAS Thematic Conference on Multibody Dynamics*, Vol. 53, p. 495, available at: https://books.google.com/books?hl=en&lr=&id=f5afDwAAQBAJ&oi=fnd&pg=PA495&ots=xPuSSGlNk8&sig=UzOISN1wP4P-nrTC-8WRBYIjt1s

Song, B., Zhang, Z., Qin, Y., Liu, X. and Hu, H. (2022), "Quantitative analysis of freight train derailment severity with structured and unstructured data", *Reliability Engineering and System Safety*, Vol. 224, p. 108563, doi: 10.1016/j.ress.2022.108563.

Tang, Z., Hu, Y., Wang, S., Ling, L., Zhang, J. and Wang, K. (2023), "Train post-derailment behaviours and containment methods: a review", *Railway Engineering Science*, doi: 10.1007/s40534-023-00313-5.

Toma, E.E. (1998), "A computer model of a train derailment", Ph.D. Thesis, M.E. Dept., Queens University, Ontario, Canada.

Transportation Safety Board of Canada (2014), "Derailment speed calculation: Montreal, Maine and Atlantic railway, train MMA-002 | date of occurrence: 06-Jul-2013 (engineering laboratory report LP039/2014; issue LP039/2014)", *Operational Services Branch*, available at: www.tsb.gc.ca/eng/lab/rail/2014/lp0392014/lp0392014.pdf

Wang, Z. and Liu, X. (2022), "Cyber security of railway cyber-physical system (CPS)–a risk management methodology", *Communications in Transportation Research*, Vol. 2, p. 100078.

Wu, Q., Luo, S. and Cole, C. (2014), "Longitudinal dynamics and energy analysis for heavy haul trains", *Journal of Modern Transportation*, Vol. 22 No. 3, pp. 127-136.

Xu, L. and Zhai, W. (2019), "A three-dimensional dynamic model for train-track interactions", *Applied Mathematical Modelling*, Vol. 76, pp. 443-465.

Zaman, A., Huang, Z., Li, W., Qin, H., Kang, D. and Liu, X. (2023), "Artificial intelligence-aided grade crossing safety violation detection methodology and a case study in New Jersey",

Transportation Research Record: Journal of the Transportation Research Board, Vol. 2677 No. 10, pp. 688-706, doi: 10.1177/03611981231163824.

Zhao, J., Dick, C.T. and Kang, D. (2023), "Analysis of derailment severity comparing unit trains at transload terminals and manifest trains at railroad switching and hump classification yards", *Transportation Research Record: Journal of the Transportation Research Board*, Vol. 2677 No. 5, pp. 793-811.

Corresponding author
Zheyong Bian can be contacted at: zbian2@central.uh.edu